

Nickel(II) Ion-Catalyzed Hydrolysis of Acetyl Esters of 2-Pyridineoxime Derivatives: Effects of Geometry around Central Metal Atom on the Efficiency of Metal Ion Catalysis

JUNGHUN SUH¹ AND BOMEI CHANG

Department of Chemistry, Seoul National University, Seoul 151, Korea

Received August 6, 1986

The kinetics of the Ni(II)-catalyzed ester hydrolysis of *O*-acetyl-2-pyridine-carboxaldoxime, *O*-acetyl-2-acetylpyridineketoxime, and *O*-acetyl-6-carboxy-2-pyridine-carboxaldoxime are measured and the values of various k_{cat} parameters are calculated for reaction paths involving one metal ion ($k_{\text{cat}}^{\text{W}}$ and $k_{\text{cat}}^{\text{OH}}$) and two metal ions ($k_{\text{cat}}^{\text{A}}$ and $k_{\text{cat}}^{\text{B}}$). Examination of the kinetic data reveals that the $k_{\text{cat}}^{\text{W}}$ and $k_{\text{cat}}^{\text{OH}}$ paths for the Ni(II)-catalyzed reactions involve the same mechanism as those for the previously reported Cu(II)-catalyzed reactions. For the $k_{\text{cat}}^{\text{A}}$ and $k_{\text{cat}}^{\text{B}}$ paths, the mechanism involving binuclear Ni(II) ions is preferred by analogy with the previously reported Zn(II)-catalyzed reactions. Comparison of $k_{\text{cat}}^{\text{OH}}$ values for the Cu(II)- and Ni(II)-catalyzed hydrolysis of 1-3 indicates that markedly different steric effects are exerted by the substituents of 2 and 3 on the catalytic behavior of the two metal ions. This is explained in terms of differences in the fit of the metal ions in the metal complexes of 1-3. Present results demonstrate that slight changes in the geometry around the central metal atom can affect the catalytic outcome significantly. The implications of the present results on metal substitution in metalloenzymes are also discussed.

© 1987 Academic Press, Inc.

Many mechanistic studies have been performed on the catalytic roles of metal ions that act as Lewis acid catalysts in organic reactions (1-3). The catalytic factors disclosed by the previous studies can be grouped into four categories (1): (i) Enhancement of the reactivity of an electrophile through attachment of the metal ion to a suitable site on the electrophile. (ii) Increase in the leaving ability of a departing nucleophile through attachment of the metal ion to the leaving group. (iii) Template effect of the metal ion acting as a center for the simultaneous attachment of both an electrophile and the attacking nucleophile, thus converting an intermolecular process into an intramolecular process. (iv) Production of improved nucleophiles through induction of ionization of protons from ambient nucleophiles by metal ions. In addition, our previous studies on the metal ion-catalyzed hydrolysis of various esters revealed novel catalytic features such as nucleophilic attack by a metal-bound water molecule at a complexed ester (4), participation by binuclear Zn(II) ions as catalytic units (5), and metal ion catalysis via blockade of inhibitory reverse paths (6).

Lewis acid catalysis by metal ions in the reactions of small organic molecules

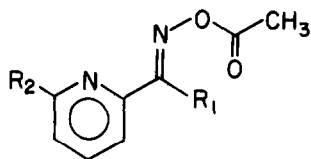
¹ To whom inquiries should be addressed.

not only provides mechanistic information on organic and inorganic reactions but also can be regarded as a model for metalloenzymes. Thus, the catalytic features disclosed by studies with small molecules can be used in the assignment of catalytic roles to the active-site metal ions of metalloenzymes.

It is very likely that active-site metal ions exert significant effects on enzymatic reactions by inducing conformational changes in the enzymes, thus bringing the catalytic groups into the right positions in the vicinity of the bound substrate (1). Although this catalytic factor has not yet been demonstrated with small model compounds, the geometry around the central metal ion of the catalytic complex should greatly influence the catalytic efficiency of both model systems and metalloenzymes.

Among metalloenzymes, carboxypeptidase A has been subjected to the most structural and mechanistic investigation (7-10). When the Zn(II) ion of native carboxypeptidase A was substituted with various metal ions, the esterase and peptidase activities of the enzyme were altered remarkably (11-17). The changes in the activities depended greatly on the nature of the substituting metal ions. Although possible configurations for the active-site metal ions of some of the substituted carboxypeptidase A's have been suggested (15, 18-20), much more detailed structures of the active sites are needed to explain the observed changes in activity. In addition to the bond angles and bond lengths involved in the interaction of the active-site metal ion with the ligand groups provided by the protein portion, properties of the metal ion, such as Lewis acidity and ligand field effects, can significantly affect the reactivity of metalloenzymes.

In model studies carried out so far, relatively little attention has been paid to the effects of geometry around central metal ions on the catalytic efficiency. In the present study, the Ni(II)-catalyzed hydrolysis of *O*-acetyl-2-pyridinecarboxaldoxime (1), *O*-acetyl-2-acetylpyridineketoxime (2), and *O*-acetyl-6-carboxy-2-pyridinecarboxaldoxime (3) has been kinetically investigated, and the results are compared with those for the corresponding reactions catalyzed by Zn(II) and Cu(II) ions which were previously studied in this laboratory (4, 5, 21, 22). In this paper, the remarkably different kinetic effects of the bivalent metal ions in the hydrolysis of 1-3 are reported, and the implications for metalloenzymes are discussed.



1: $R_1 = H, R_2 = H$

2: $R_1 = CH_3, R_2 = H$

3: $R_1 = H, R_2 = COOH$

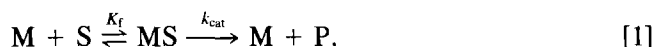
EXPERIMENTAL PROCEDURES

Materials. Substrates 1-3 were prepared according to methods described in the literature (5, 21, 22). Solutions of nickel chloride were prepared by dissolving nickel oxide (Aldrich "Gold Label") with hydrochloric acid. Water was distilled and deionized prior to use in the kinetic studies.

Kinetic measurements. Reaction rates were measured with a Beckman 5260 or 25 UV/vis spectrophotometer. Temperature was controlled at $25 \pm 0.1^\circ\text{C}$ with a Haake E52 circulator. pH measurements were carried out with a Fisher Accumet 525 pH meter. Kinetics were measured at an ionic strength of 1.0, which was adjusted with sodium chloride. Either 4-morpholinoethanesulfonic acid (pH 6.2–7.2) or *N*-(2-hydroxyethyl)piperazine-*N'*-2-ethanesulfonic acid (pH 6.8–7.8) was used as buffer. Stock solutions of the substrates were made in dimethyl sulfoxide; reaction mixtures for kinetic studies contained 0.8% (v/v) dimethyl sulfoxide. The initial concentration of the substrates was 1×10^{-4} M. The reaction was followed spectrophotometrically for the release of Ni(II) complexes of the oxime moieties. Production of the oximes in quantitative yields was evidenced by the product spectra obtained at various pHs. Pseudo-first-order rate constants (k_0) were calculated with the infinity absorbance readings measured.

RESULTS

The k_0 values measured for **1** and **2** in the presence of Ni(II) ion manifested saturation kinetic behavior with respect to [Ni(II)]. This has been also observed in the Cu(II)-catalyzed hydrolysis of **1**, and indicates that the metal ion-catalyzed hydrolysis proceeds through the formation of metal–substrate complexes (4). Thus, the saturation kinetic data were analyzed in terms of



Here, K_f represents the formation constant for MS (metal–substrate complex), and k_{cat} , the first-order rate constant for the conversion of MS to the product. The rate expression of Eq. [1] is

$$k_0 = k_{\text{cat}}[\text{M}]/(1/K_f + [\text{M}]) \quad [2]$$

which is linearly transformed into

$$1/k_0 = (1/k_{\text{cat}}K_f)(1/[\text{M}]) + 1/k_{\text{cat}}. \quad [3]$$

From the slopes and intercepts of the linear plots of $1/k_0$ against $1/[\text{M}]$, the values of k_{cat} and K_f were measured for **1** at pH 6.78–7.66 and for **2** at pH 6.29–7.16. The K_f values were not greatly affected by pH as was observed with the Cu(II)-catalyzed hydrolysis (4) of **1**. The k_{cat} values depended systematically on $[\text{OH}^-]$ as illustrated in Figs. 1 and 2. Thus, k_{cat} is a linear function of $[\text{OH}^-]$ as indicated by

$$k_{\text{cat}} = k_{\text{cat}}^{\text{W}} + k_{\text{cat}}^{\text{OH}}[\text{OH}^-]. \quad [4]$$

The values of the kinetic parameters obtained for the Ni(II)-catalyzed hydrolysis of **1** and **2** are summarized in Table 1.

Substrate **3** is completely bound to Ni(II) ion even at 2 mM Ni(II), as illustrated in Fig. 3. Thus, the value of K_f for the Ni(II) · **3** complex is much greater than 500 M^{-1} . The k_0 values were measured under the condition of complete complexation of **3** to Ni(II). The k_0 values thus obtained at pH 6.8–7.8 were linearly dependent

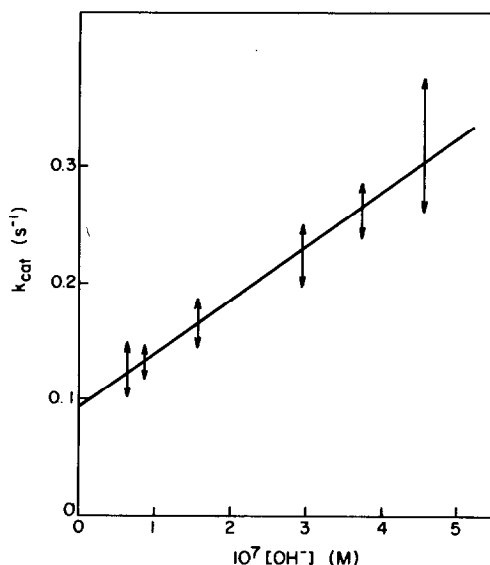


FIG. 1. The plot of k_{cat} against $[\text{OH}^-]$ for the Ni(II)-catalyzed hydrolysis of **1**. The straight line was obtained by weighted linear regression.

TABLE I
VALUES OF KINETIC PARAMETERS FOR THE HYDROLYSIS OF **1**–**3** CATALYZED BY VARIOUS
BIVALENT METAL IONS^a

Substrate	Catalyst		
	Zn(II)	Cu(II)	Ni(II)
1	$k_{\text{cat}}^{\text{OH}} K_f = 1.7 \times 10^6 \text{ M}^{-2} \text{ s}^{-1}$ ($K_f \leq 5 \text{ M}^{-1}$)	$k_{\text{cat}}^{\text{W}} = 1.7 \times 10^{-2} \text{ s}^{-1}$ $k_{\text{cat}}^{\text{OH}} = 3.0 \times 10^8 \text{ M}^{-1} \text{ s}^{-1}$ ($K_f = 70 \text{ M}^{-1}$)	$k_{\text{cat}}^{\text{W}} = 9.2 \times 10^{-2} \text{ s}^{-1}$ $k_{\text{cat}}^{\text{OH}} = 4.5 \times 10^5 \text{ M}^{-1} \text{ s}^{-1}$ ($K_f = 70 \text{ M}^{-1}$)
2	$k_{\text{cat}}^{\text{W}} K_f = 4.5 \times 10^{-2} \text{ M}^{-1} \text{ s}^{-1}$ $k_{\text{cat}}^{\text{OH}} K_f = 1.5 \times 10^7 \text{ M}^{-2} \text{ s}^{-1}$ $k_{\text{cat}}^{\text{B}} K_f = 4.1 \times 10^{16} \text{ M}^{-4} \text{ s}^{-1}$ ($K_f \leq 5 \text{ M}^{-1}$)	Too fast to measure ^b	$k_{\text{cat}}^{\text{OH}} = 7.0 \times 10^5 \text{ M}^{-1} \text{ s}^{-1}$ ($K_f = 1200 \text{ M}^{-1}$)
3^c	$k_{\text{cat}}^{\text{A}} = 1.3 \times 10^6 \text{ M}^{-2} \text{ s}^{-1}$ $k_{\text{cat}}^{\text{B}} = 3.9 \times 10^{13} \text{ M}^{-3} \text{ s}^{-1}$	Extremely slow ^d	$k_{\text{cat}}^{\text{OH}} = 1.4 \times 10^3 \text{ M}^{-1} \text{ s}^{-1}$ $k_{\text{cat}}^{\text{A}} = 2.4 \times 10^4 \text{ M}^{-2} \text{ s}^{-1}$ $k_{\text{cat}}^{\text{B}} = 1.1 \times 10^{11} \text{ M}^{-3} \text{ s}^{-1}$

^a Data for the Zn(II)- and Cu(II)-catalyzed reactions were taken from Refs. (4, 5, 21, 22).

^b The reaction was complete within the period of manual mixing (<5 s) at pH 2 in the presence of 1 mM Cu(II), with the half-life being smaller than 1 s. On the other hand, the half-life for the hydrolysis of **1** was about 40 s at pH 2–3 under the condition of complete binding of **1** to Cu(II).

^c Complete binding of **3** to metal ions was observed even at 2 mM Zn(II), Cu(II), or Ni(II).

^d No reaction was observed for 12 h at pH 4 under the condition of full binding of the substrate to Cu(II) ion.

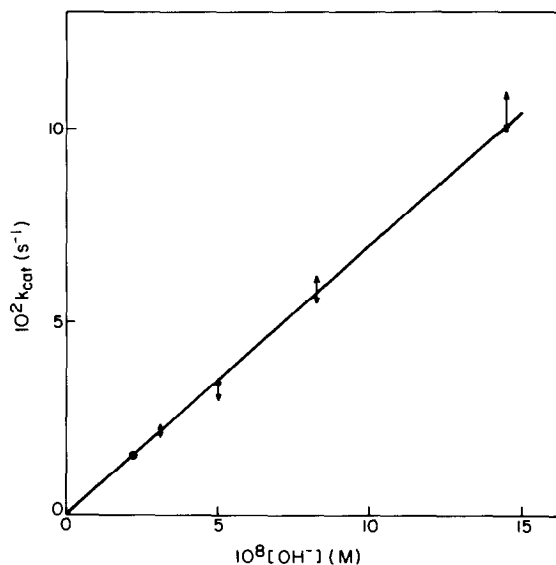


FIG. 2. The plot of k_{cat} against $[\text{OH}^-]$ for the Ni(II)-catalyzed hydrolysis of **2**. The intercept obtained by weighted linear regression is $(4.7 \pm 8.1) \times 10^{-4} \text{ s}^{-1}$.

on $[\text{Ni(II)}]$ as illustrated in Fig. 4. The intercepts (k_{int}) of the lines drawn in Fig. 4 are proportional to $[\text{OH}^-]$, as illustrated in Fig. 5. The logarithmic values of the slopes (k_{sl}) of the lines drawn in Fig. 4 are pH dependent, as illustrated in Fig. 6, which is not readily analyzed. Instead, $k_{\text{sl}}/[\text{OH}^-]$ is linearly dependent on $[\text{OH}^-]$, as illustrated in Fig. 7.

Since **3** is completely converted into the $\text{Ni(II)} \cdot \text{3}$ complex under the conditions of the kinetic measurements, the k_{int} value obtained from the lines in Fig. 4

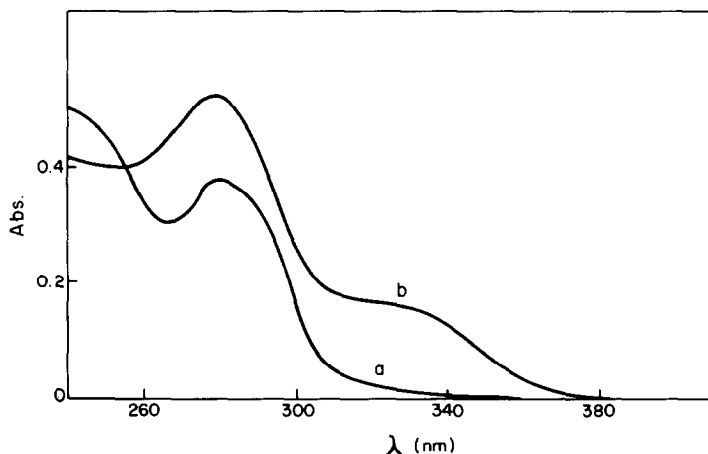


FIG. 3. Ultraviolet spectrum of **3** ($1.0 \times 10^{-4} \text{ M}$) measured at pH 7.41 in the absence (curve a) or presence (curve b) of 2–16 mM Ni(II).

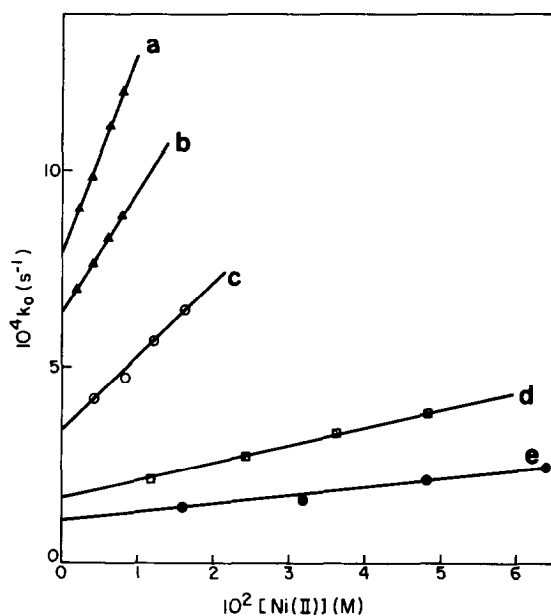


FIG. 4. The plot of k_0 against $[\text{Ni(II)}]$ for the Ni(II) -catalyzed hydrolysis of **3** measured at pH 7.77 (a), 7.66 (b), 7.41 (c), 7.10 (d), and 6.80 (e).

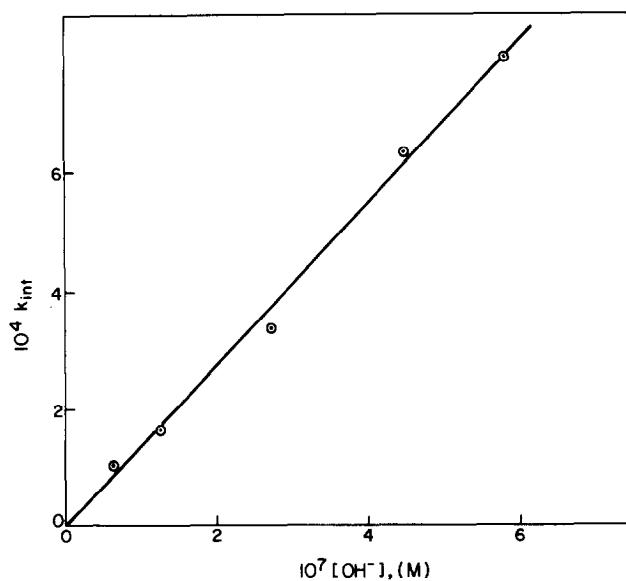


FIG. 5. The plot of the intercepts (k_{int}) of the straight lines obtained in Fig. 4 against $[\text{OH}^-]$. The intercept of the line indicated in this figure obtained by weighted linear regression is $(-2.26 \pm 2.05) \times 10^{-5} \text{ s}^{-1}$.

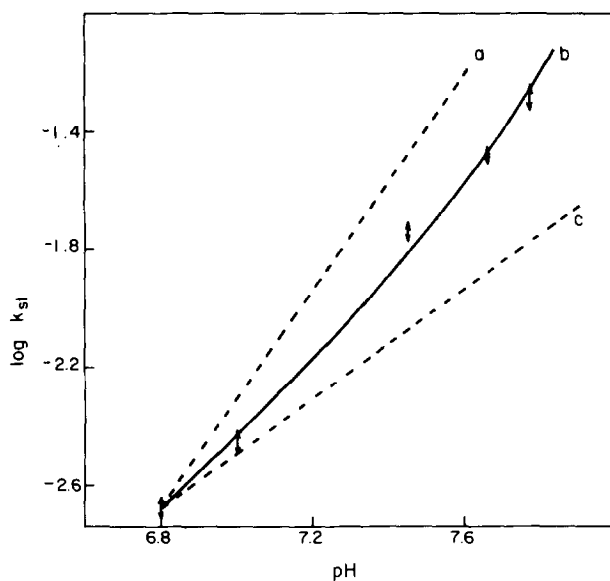


FIG. 6. The plot of the logarithmic values of the slopes (k_s) of the straight lines obtained in Fig. 4 against pH. Curve b is constructed on the basis of Eq. [9] and parameter values listed in Table 1. Lines a and c are drawn with slopes 2 and 1, respectively.

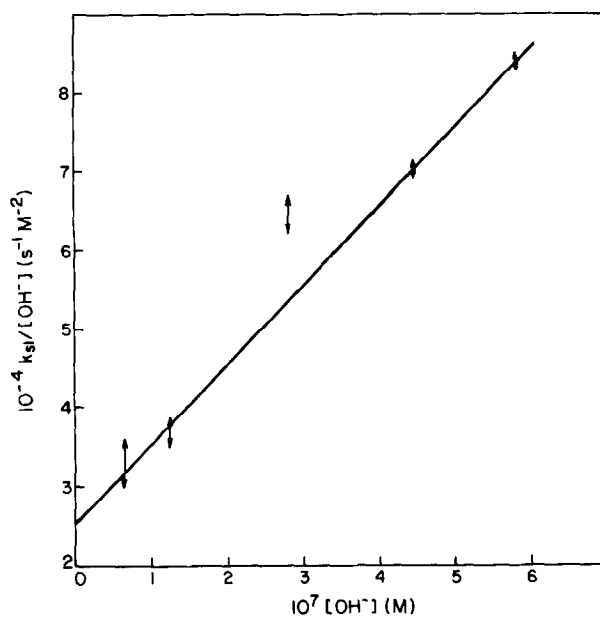


FIG. 7. The plot of $k_s/[\text{OH}^-]$ against $[\text{OH}^-]$ for the Ni(II)-catalyzed hydrolysis of 3. The straight line was obtained by weighted linear regression.

represents the conversion of $\text{Ni(II)} \cdot \mathbf{3}$ into products without the assistance of an additional Ni(II) ion. The corresponding k_{sl} values stand for the reaction of $\text{Ni(II)} \cdot \mathbf{3}$ complex with the participation of an extra Ni(II) ion, as observed in the Zn(II) -catalyzed hydrolysis of $\mathbf{3}$ (5). These are best explained by the scheme in



The rate expression for Eq. [5] is

$$k_0 = (k_{\text{cat}}^0 + k_{\text{cat}}^{\text{M}}[\text{M}])[\text{M}]/(1/K_f + [\text{M}]). \quad [6]$$

Under the conditions of $[\text{M}] \gg 1/K_f$, Eq. [6] becomes

$$k_0 = k_{\text{cat}}^0 + k_{\text{cat}}^{\text{M}}[\text{M}] \quad [7]$$

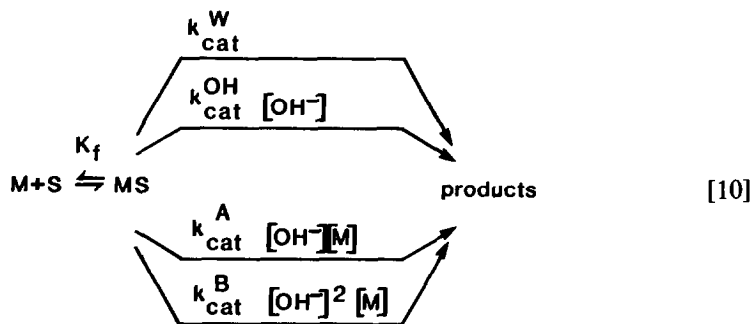
resulting in the kinetic behavior illustrated in Fig. 4. Thus, k_{cat}^0 and $k_{\text{cat}}^{\text{M}}$ correspond to k_{int} and k_{sl} , respectively, estimated from the lines illustrated in Fig. 4. Dependence of k_{int} and k_{sl} on $[\text{OH}^-]$ further leads to the equations

$$k_{\text{int}} = k_{\text{cat}}^0 = k_{\text{cat}}^{\text{OH}}[\text{OH}^-] \quad [8]$$

$$k_{\text{sl}} = k_{\text{cat}}^{\text{M}} = k_{\text{cat}}^{\text{A}}[\text{OH}^-] + k_{\text{cat}}^{\text{B}}[\text{OH}^-]^2 \quad [9]$$

The values of the kinetic parameters in Eqs. [8] and [9] ($k_{\text{cat}}^{\text{OH}}$, $k_{\text{cat}}^{\text{A}}$, and $k_{\text{cat}}^{\text{B}}$) estimated from the kinetic data for the Ni(II) -catalyzed hydrolysis of $\mathbf{3}$ are summarized in Table 1.

The hydrolysis of ester substrates $\mathbf{1}$ – $\mathbf{3}$ catalyzed by Zn(II) , Cu(II) , and Ni(II) can be summarized by the scheme



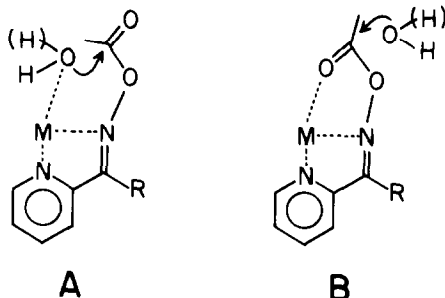
The values of the kinetic parameters measured for each substrate in the presence of various metal ions are compared in Table 1.

DISCUSSION

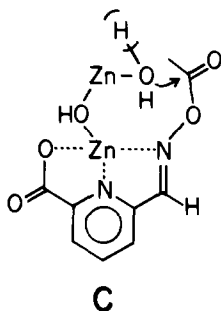
Mechanisms for the Ni(II)-Catalyzed Hydrolysis of 1–3

Two mechanisms have been proposed for the Zn(II) - or Cu(II) -catalyzed hydrolysis of $\mathbf{1}$ and $\mathbf{2}$: **A** and **B** (4, 22). Mechanism **A** assumes the intramolecular attack of the metal-bound water molecule or hydroxide ion at the complexed

ester; mechanism **B** assumes polarization of the scissile carbonyl bond, in addition to an increase in the leaving group ability of the oximate anion.



For the Cu(II)-catalyzed hydrolysis of **1** and **2**, k_{cat} values were separately estimated from the kinetic data. Detailed mechanistic analysis of the k_{cat} values indicated that **A** is the correct mechanism (4, 22). For the Zn(II)-catalyzed hydrolysis of **1** and **2**, $k_{\text{cat}}K_f$ values were experimentally determined because the small K_f values did not allow the separate estimation of k_{cat} (21, 22).² In the Zn(II)-catalyzed hydrolysis of **2**, a new reaction path whose rate was proportional to $[\text{Zn(II)}]^2[\text{OH}^-]^2$ was observed, although it was not clear whether the reaction path involved two separate hydroxozinc(II) ions or a binuclear Zn(II) ion as the catalytic species (22). To differentiate these possibilities, the Cu(II)- and Zn(II)-catalyzed hydrolysis of **3** was investigated (5). In the presence of Cu(II) ion, the reaction of **3** was not detected, in contrast to the rapid rates of the Cu(II)-catalyzed hydrolysis of **1** and **2**. In the Zn(II)-catalyzed hydrolysis of **3**, reaction paths represented by $k_{\text{cat}}^{\text{A}}$ and $k_{\text{cat}}^{\text{B}}$ were observed, whereas those represented by $k_{\text{cat}}^{\text{W}}$ and $k_{\text{cat}}^{\text{OH}}$ were absent. Detailed analysis of the kinetic data indicated that the $k_{\text{cat}}^{\text{A}}$ and $k_{\text{cat}}^{\text{B}}$ paths were consistent with the mechanisms in which binuclear Zn(II) ions are involved as catalytic units (**C**) (5).³



² Although mechanistic analysis was not based on separately estimated values of k_{cat} for the Zn(II)-catalyzed hydrolysis of **1** and **2**, it is highly likely that the $k_{\text{cat}}^{\text{W}}$ and $k_{\text{cat}}^{\text{OH}}$ paths in these reactions can be assigned to mechanism **A** since the corresponding reactions catalyzed by both Cu(II) and Ni(II) ions (as discussed in the later part of the Discussion) involve the same mechanism. The mechanism for the Zn(II)-catalyzed hydrolysis of **3**, however, has been determined by using the measured values of k_{cat} .

³ The kinetic data do not indicate the exact nature (e.g., positions of protons) of the bridging ligand (5). Likewise, it is also possible that the reaction proceeds through polarization of the carbonyl group by its coordination to the terminal metal ion of the binuclear metal ion (e.g., mechanism **N**).

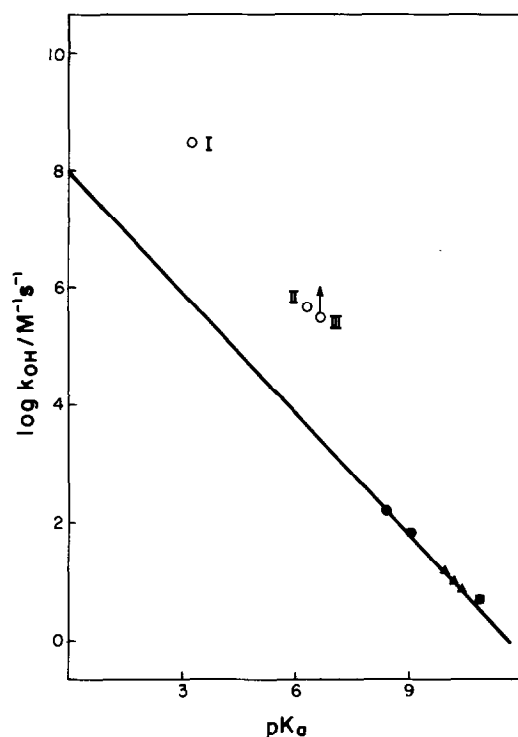
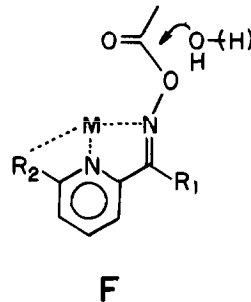
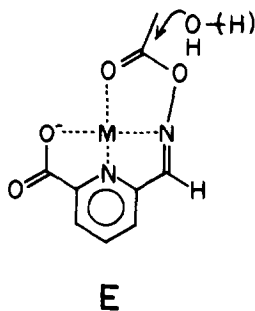
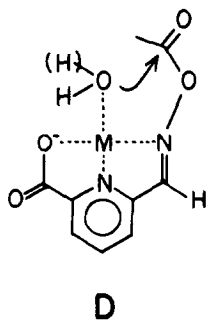


FIG. 8. The plot of the logarithmic values of the second-order rate constants against pK_a of leaving oximes for the alkaline hydrolysis of acetyl esters of various oximes. The pK_a (6.3) of the Ni(II) complex of 2-pyridinecarboxaldoxime was measured in the present study by spectral titration. The data points, except that for Ni(II) · 1 complex (II), are reported in the literature (4, 21) for the acetyl esters of bezaloxime (■), 2-, 3-, or 4-pyridinecarboxaldoxime (▲), and 3- or 4-(hydroxyimino)-methyl-*N*-methylpyridinium internal salt (●) in addition to Cu(II) · 1 (I) and Zn(II) · 1 (III) complexes.

1. k_{cat}^w and k_{cat}^{OH} paths. In Ni(II)-catalyzed reactions, the k_{cat} values were separately measured and a detailed mechanistic analysis was performed by using these values. Mechanisms **A** and **B** and their extended forms **D** and **E** can be considered as candidates for the k_{cat}^w and k_{cat}^{OH} paths of the Ni(II)-catalyzed hydrolysis of 1–3. In addition, mechanism **F**, which assumes only an increase in the leaving ability of



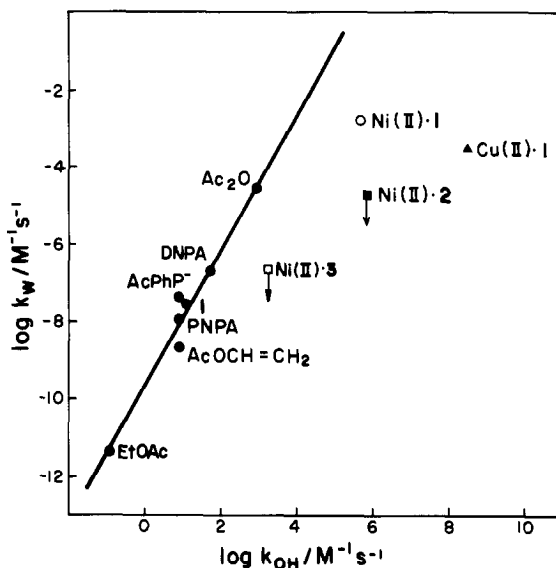


FIG. 9. The plot of the logarithmic values of the second-order rate constants (k_W) for the water attack against those (k_{OH}) for the hydroxide attack in the hydrolysis of various acetyl derivatives. The data points, except those for the Ni(II) complexes, are taken from the literature (4) (DNPA; 2,4-dinitrophenyl acetate, AcPhP^- ; acetyl phenyl phosphate anion, PNPA; *p*-nitrophenyl acetate). Upper limits of k_W for Ni(II) · 2 and Ni(II) · 3 are estimated by assuming the intercepts of Fig. 2 and 5 as 1×10^{-3} and $1 \times 10^{-5} \text{ s}^{-1}$ (see the respective figure legends), respectively. The k_{cat}^W values for the metal ion-catalyzed reactions are divided by 55 M to obtain the respective bimolecular rate constants k_W .

the oximate anion, is a possible mechanism for the Ni(II)-catalyzed reactions. In Fig. 8, the logarithmic values of the second-order rate constants for the alkaline hydrolysis of various acetyl oxime esters are plotted against the $\text{p}K_a$ values of the leaving oximes. The line drawn in this figure predicts the alkaline rates when only the $\text{p}K_a$ of the oxime group is affected. The large deviation observed for Ni(II), Cu(II), and Zn(II) complexes with **1** indicates that additional catalytic factors, such as those illustrated in **A**, **B**, **D**, and **E**, are needed to explain the observed rates (21). Thus, mechanism **F** can be excluded.

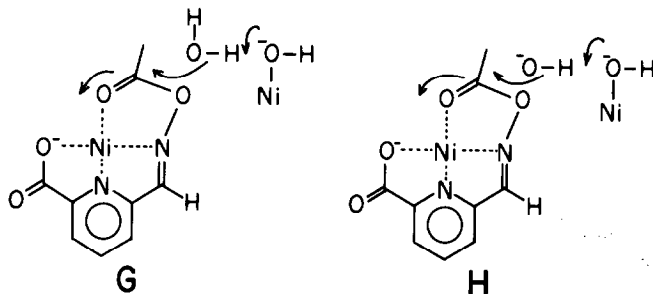
To differentiate **A** from **B** as the mechanism for the k_{cat}^W and $k_{\text{cat}}^{\text{OH}}$ paths in the Cu(II)-catalyzed hydrolysis of **1**, the reactivity–selectivity relationship illustrated in Fig. 9 has been used (4).⁴ In **B**, a hydroxide ion or a water molecule attacks as an external nucleophile at an acetyl derivative. As the acetyl substrate becomes more reactive, the selectivity manifested by the substrate toward the hydroxide ion and the water molecule should decrease. For the various acetyl substrates illustrated in Fig. 9, the plot of $\log k_W$ against k_{OH} measured in the absence of any metal ion catalyst is a straight line. The slope (1.73) of the line is greater than 1,

⁴ The steric compression in the transition state by the methyl group of **2**, which was inferred from the much greater k_{cat} values for **2** compared with **1** in the Cu(II)-catalyzed hydrolysis reactions, has been also used as evidence for mechanism **A** (22).

indicating that the ratio $k_{\text{OH}}/k_{\text{w}}$ becomes smaller and, consequently, the selectivity decreases as the substrate becomes more reactive.

The data point for the $\text{Cu(II)} \cdot \mathbf{1}$ complex indicated in Fig. 9 was based on a calculation assuming mechanism **B**. The deviation of this data point indicates that the $\text{Cu(II)} \cdot \mathbf{1}$ complex should be much more selective toward hydroxide ion although it is much more reactive than the other substrates, if mechanism **B** is assumed. Similarly, the data points for the $\text{Ni(II)} \cdot \mathbf{1}$, $\text{Ni(II)} \cdot \mathbf{2}$, and $\text{Ni(II)} \cdot \mathbf{3}$ complexes deviate markedly from the straight line, strongly suggesting that the Ni(II) -catalyzed hydrolysis of **1–3** and the spontaneous hydrolysis of the other acetyl substrates do not involve common nucleophiles, water molecule and hydroxide ion. Then, mechanism **A/D** is much more reasonable than **B/E** for the $k_{\text{cat}}^{\text{w}}$ and $k_{\text{cat}}^{\text{OH}}$ paths in the Ni(II) -catalyzed hydrolysis of **1–3** as well as in the Cu(II) -catalyzed reaction.⁵

2. $k_{\text{cat}}^{\text{A}}$ and $k_{\text{cat}}^{\text{B}}$ paths. Mechanisms **G** and **H** may be considered as possible mechanisms for the $k_{\text{cat}}^{\text{A}}$ and $k_{\text{cat}}^{\text{B}}$ paths of the Ni(II) -catalyzed hydrolysis of **3**. In **G** and **H**, a second hydroxoxonickel(II) ion participates as a general base in the reaction paths represented by **E**. Since **E** has been excluded as a mechanism for the $k_{\text{cat}}^{\text{w}}$ and $k_{\text{cat}}^{\text{OH}}$ paths, it is not likely that **G** and **H** are operative in the $k_{\text{cat}}^{\text{A}}$ and $k_{\text{cat}}^{\text{B}}$ paths. In addition, **H** assumes that the attack by the hydroxide ion is assisted by a much weaker base [$\text{p}K_{\text{a}}$ of $\text{Ni(II)} \cdot \text{H}_2\text{O} = 10.6$ (23)], which is not probable.

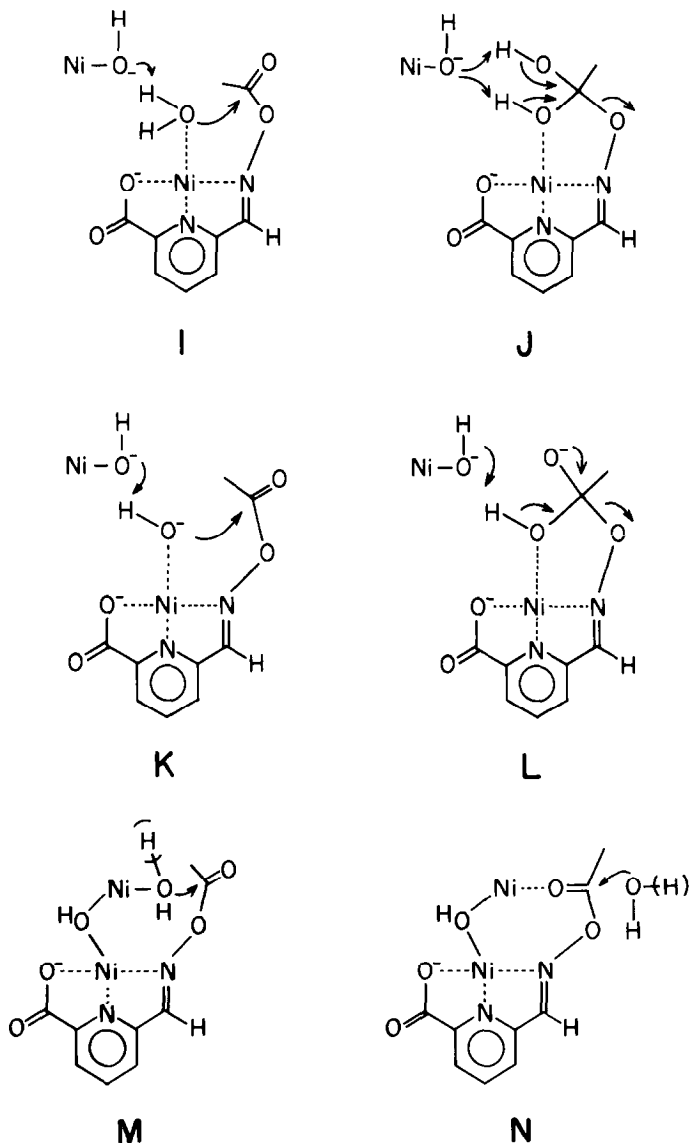


If the additional hydroxoxonickel(II) ion participates as a general base in the mechanism of **D**, the $k_{\text{cat}}^{\text{A}}$ and $k_{\text{cat}}^{\text{B}}$ paths may be assigned to mechanisms **I/J** and **K/L**, respectively, depending on the nature (22) of the rate-determining step. The possibility of general base catalysis in the attack of the metal-bound water molecule as in **I/J** has been discussed (4).⁶ Mechanisms **K/L** are analogous to those

⁵ The k_{w} value for $\text{Ni(II)} \cdot \mathbf{1}$ is much greater than that for $\text{Ni(II)} \cdot \mathbf{2}$, while the respective k_{OH} values are comparable to each other as illustrated in Fig. 9. The water and hydroxide paths may involve different rate-determining steps (22). In addition, the water path appears to involve the participation of an additional water molecule as a general base (4). It is further possible that more than one metal-bound water molecule is involved in the network of water molecules in the general base-assisted reaction of the water path. The much greater k_{w} for $\text{Ni(II)} \cdot \mathbf{1}$ could be explained in terms of steric and electronic effects on these aspects, but an analysis is not easily performed at present.

⁶ Kinetic studies of the Ni(II) -catalyzed hydrolysis of **3** in the presence of various general bases were not successful due to interaction of the added general bases with the metal ion. When biphosphate was used as a buffer at pH 6.8, Ni(II) ion precipitated, apparently due to the formation of less soluble salts with the buffer anion. The pH of buffer solutions containing Ni(II) and bicarbonate ions drifted to higher values, apparently due to the decomposition of carbonic acid catalyzed by Ni(II) . When imidazole was used as buffer, it formed complexes with Ni(II) ion as indicated by a color change from green to blue.

proposed for the bimolecular participation of amines in the aminolysis of esters or for the bimolecular participation of hydroxide ion in the alkaline hydrolysis of anilides (22).



In the $k_{\text{cat}}^{\text{A}}$ and $k_{\text{cat}}^{\text{B}}$ paths of the Zn(II) -catalyzed hydrolysis of **3**, several lines of evidence have been obtained in support of mechanism **C** (5). Analogous mechanisms **M/N** are also consistent with the kinetic data obtained for the $k_{\text{cat}}^{\text{A}}$ and $k_{\text{cat}}^{\text{B}}$ paths of the Ni(II) -catalyzed hydrolysis of **3**.³ Although it is not possible to differentiate mechanisms **M/N** from **I-L** rigorously, **M/N** might be preferred by analogy with the Zn(II) -catalyzed reaction. In this regard, it is noteworthy that the mechanisms for the $k_{\text{cat}}^{\text{W}}$ and $k_{\text{cat}}^{\text{OH}}$ paths are identical for the catalysis by bivalent metal ions Cu(II) and Ni(II) , as discussed above.

Different Effects of Cu(II) and Ni(II)

A comparison can readily be made between catalysis by Cu(II) ion and catalysis by Ni(II) ion in the $k_{\text{cat}}^{\text{W}}$ and $k_{\text{cat}}^{\text{OH}}$ paths since identical mechanisms are operative in these paths and k_{cat} values are available for both metal ions. The most marked difference in the effects exerted by Cu(II) and Ni(II) ions is the extremely large difference in rates for the Cu(II)-catalyzed reactions of **1–3** compared with the relatively small variation in the rates for the Ni(II)-catalyzed reactions. In the Cu(II)-catalyzed hydrolysis, the k_{cat} values are much greater for **2** compared with **1**, and much smaller for **3** compared with **1**. On the contrary, the differences in the $k_{\text{cat}}^{\text{OH}}$ values⁷ for the Ni(II)-catalyzed hydrolysis of **1–3** are not as large as those in the k_{cat} values for the Cu(II)-catalyzed reactions.

The large rate enhancement caused by the introduction of the methyl substituent in **2** in the Cu(II)-catalyzed reaction has been attributed to the steric compression of the transition state for **A** by the methyl substituent (22).⁴ Similarly, the large rate retardation resulting from the incorporation of the carboxyl group in **3** in Cu(II)-catalyzed hydrolysis has been interpreted in terms of the steric expansion in the transition state of **D** by the carboxyl group (5). A five-membered ring which is absent in the ground state is formed in the transition state of mechanism **A**. The nonbonded interaction of the methyl group of **2** with the acyl moiety and with the adjacent hydrogen of the pyridine ring would push the carbonyl carbon toward the metal-bound nucleophile oxygen atom. The consequent steric compression can stabilize the transition state. On the other hand, the carboxyl group of **3** could hold back the central metal ion of mechanism **D**, increasing the distance between the metal-bound nucleophile atom and the carbonyl carbon. This can lead to the destabilization of the transition state for mechanism **D** and the near-total disappearance of hydrolysis of **3**.

If the interpretations of the Cu(II)-catalyzed reactions are valid, the relatively small variation in $k_{\text{cat}}^{\text{OH}}$ values for the Ni(II)-catalyzed hydrolysis of **1–3** suggests that steric compression and expansion are less important when the central atom is Ni(II). This difference between the two metal ions is related to the relative stabilities of the reactants and the rate-determining transition states. The common configurations of Cu(II) and Ni(II) complexes are octahedral, trigonal bipyramidal, square pyramidal, tetrahedral, and square planar, depending on coordination number (24). Moreover, the octahedral and tetrahedral configurations for Cu(II) complexes are distorted due to the Jahn–Teller effect. It is, however, impossible at present to determine the configuration around the central metal ion and the structural dimensions associated with it in the metal complexes of **1–3** and the corresponding tetrahedral intermediates in aqueous solutions.

The different steric effects of **1–3** on the kinetic behavior of Cu(II) and Ni(II) ions might be explained by assuming that Cu(II) ion fits less tightly into the complex formed with the substrates compared with Ni(II) ion. The looser fit of Cu(II) ion can lead to the greater sensitivity of rates for the Cu(II)-catalyzed

⁷ Since the $k_{\text{cat}}^{\text{W}}$ value was accurately measured only for **1** in the Ni(II)-catalyzed hydrolysis, comparison of kinetic parameters for the Ni(II)-catalyzed hydrolysis of **1–3** can be performed most meaningfully with $k_{\text{cat}}^{\text{OH}}$.

reactions to steric effects. The better fit of Ni(II) compared with Cu(II) in the complexes formed with **1** is supported by identical K_f values for Cu(II) · **1** and the Ni(II) · **1** complexes (Table 1). Since Ni(II) is a weaker Lewis acid than Cu(II) (Irving–Williams order) (1, 23–26),⁸ the K_f for Ni(II) · **1** would be much smaller than that for Cu(II) · **1** unless Ni(II) fits more snugly in the chelate ring system.

In the Cu(II)- or Ni(II)-catalyzed hydrolysis of **1–3**, a change in the nature of the central metal ion would lead to relatively small changes in the structure of the metal complexes of the substrates and the transition states compared with enzymatic systems. In the action of metalloenzymes, the transition states are much more ordered than those for **1–3**, involving many interactions among the active-site metal ion, the protein moiety of the enzyme, and the bound substrate.⁹ It is easily predicted that the geometry around the active-site metal ion exerts crucial effects on the enzyme activity. It is, however, almost impossible to elucidate the detailed mechanistic changes accompanying metal substitution in a metalloenzyme by using currently available techniques. In this regard, the present study can be considered as a model for the importance of the geometry around the active-site metal ion in enzyme activity. The present results indicate that minute changes in geometry around the central metal ion can result in marked differences in the kinetic behavior of small compounds. In metalloenzymes, substitution of the active-site metal ion with other metal ions would be accompanied by compounded changes in a number of chemical properties. Further extensive model studies are therefore needed to understand the effects of metal substitution in metalloenzymes.

ACKNOWLEDGMENT

This work was supported by a grant from the Korea Science and Engineering Foundation.

REFERENCES

1. SACHELL, D. P. N., AND SACHELL, R. S. (1979) *Annu. Rep. Progr. Chem. Sect. A* **75**, 25 and references therein.
2. DUNN, M. F. (1975) *Struct. Bond.* **23**, 61.
3. HIPPEL, C. J., AND BUSCH, D. H. (1978) *Coordination Chemistry* (Martell, A. E., Ed.), Vol. 2, Chap. 2, Monograph 174, Amer. Chem. Soc., Washington, DC.
4. SUH, J., CHEONG, M., AND SUH, M. P. (1982) *J. Amer. Chem. Soc.* **104**, 1654.
5. SUH, J., HAN, O., AND CHANG, B. (1986) *J. Amer. Chem. Soc.* **108**, 1839.
6. SUH, J., AND CHUN, K. H. (1986) *J. Amer. Chem. Soc.* **108**, 3057.
7. LIPSCOMB, W. N. (1974) *Tetrahedron* **30**, 1725 and references therein.

⁸ The pK_a of the oxime group in the Ni(II) complex of 2-pyridinecarboxaldoxime is 6.3, whereas that of the corresponding Cu(II) complex is 3.2 as indicated in Fig. 9. This also supports the greater Lewis acidity of Cu(II) compared with Ni(II).

⁹ In carboxypeptidase A, for example, the active-site Zn(II) ion coordinates to His-69, Glu-72, and His-196, and further interacts with the carbonyl group of the substrate. In addition, Arg-145, Tyr-248, and Glu-270 participate in catalysis during the process of ester or amide hydrolysis of the substrates (7).

8. PRINCE, R. H. (1979) *Adv. Inorg. Chem. Radiochem.* **22**, 349.
9. SUH, J., CHO, W., AND CHUNG, S. (1985) *J. Amer. Chem. Soc.* **107**, 4530.
10. SUH, J., HONG, S.-B., AND CHUNG, S. (1986) *J. Biol. Chem.* **261**, 7112.
11. COLEMAN, J. E., AND VALLEE, B. L. (1961) *J. Biol. Chem.* **236**, 2244.
12. COLEMAN, J. E., PULIDO, P., AND VALLEE, B. L. (1966) *Biochemistry* **5**, 2019.
13. DAVIES, R. C., RIORDAN, J. F., AULD, D. S., AND VALLEE, B. L. (1968) *Biochemistry* **7**, 1090.
14. KANG, E. P., STORM, C. B., AND CARSON, F. W. (1972) *Biochem. Biophys. Res. Commun.* **49**, 621.
15. DEKOCHE, R. J., WEST, D. J., CANNON, J. C., AND CHASTEEN, N. R. (1974) *Biochemistry* **13**, 4347.
16. AULD, D. S., AND HOLMQUIST, B. (1974) *Biochemistry* **13**, 4352.
17. SCHÄFFER, A., AND AULD, D. S. (1986) *Biochemistry* **25**, 2476.
18. LATT, S. A., AND VALLEE, B. L. (1971) *Biochemistry* **10**, 4263.
19. ROSENBERG, R. C., ROOT, C. A., WANG, R. H., GERDONIO, M., AND GRAY, H. B. (1973) *Proc. Natl. Acad. Sci. USA* **70**, 161.
20. ROSENBERG, R. C., ROOT, C. A., AND GRAY, H. B. (1975) *J. Amer. Chem. Soc.* **97**, 21.
21. SUH, J., LEE, E., AND JANG, E. S. (1981) *Inorg. Chem.* **20**, 1932.
22. SUH, J., AND HAN, H. (1984) *Bioorg. Chem.* **12**, 177.
23. BASOLO, F., AND PEARSON, R. G. (1968) *Mechanisms of Inorganic Reactions*, 2nd ed. pp. 32 and 80, Wiley, New York.
24. COTTON, F. A., AND WILKINSON, G. (1972) *Advanced Inorganic Chemistry*, 3rd ed., p. 596 and Chap. 25, Wiley, New York.
25. IRVING, H., AND WILLIAMS, R. J. P. (1953) *J. Chem. Soc.*, 3192.
26. YATSIMIRSKII, K. B., AND VASIL'EV, V. P. (1960) *Instability Constants of Complex Compounds*, Engl. ed., p. 81, Pergamon, London.
27. SUH, J., SUH, M. P., AND LEE, J. D. (1985) *Inorg. Chem.* **24**, 3088.